Validation Data for Ion Thruster Beam Optics Simulation

IEPC-2011-055

Presented at the 32nd International Electric Propulsion Conference,
Wiesbaden • Germany
September 11 – 15, 2011

Yoshinori Nakayama[1]
National Defense Academy of Japan, Yokosuka, Kanagawa 239-8686, Japan

Abstract: For development of more precise numerical estimation of ion thruster durability, both precise ion beam optics code and various validation data for its code are necessary. In order to obtain the validation data, in this study, plasma sheath edges and ion beam optics with various net acceleration voltages were visually measured, with a two-dimensional ion thruster. Since the experimental data was in good agreement with electrostatic acceleration theory, the obtained data was useful for the validation and the development.

Nomenclature

e	=	elementary electric charge
I_{ac}	=	acceleration grid current
I_b	=	ion beam current
I_{sc}	=	screen grid current
J_{pi}	=	ion saturation current density
J_{si}	=	space charge limited current density
k	=	Boltzmann constant
L	=	electrostatic acceleration length
M	=	propellant mass
n_p	=	plasma number density
T_e	=	electron temperature
V	=	electric potential gap
V_n	=	net acceleration voltage
x,y,z	=	position
ε_0	=	permittivity of vacuum

I. Introduction

ION thrusters are expected to increase in number and variety, because they has an attractive thruster performance for station keeping and interplanetary mission spacecraft. One of the attractive performances is durability. General ion thruster can operate over a year. For development of such a durable thruster, precise numerical analysis is useful and/or indispensable tool to confirm its durability because experimental confirmation demands high costs and a long time. Many numerical analyses have been studied as design aids for ion thrusters.[1-7)] Nevertheless, numerical analysis codes have not been completed. Reasons include the greater difficulty of a numerical model inspection and validation. Numerical analysis derives not only current data but also shape of ion beam optics, however, most validations were performed with the only grid current changes, so far. Furthermore, the data were not common data but unique data obtained by the researcher selves. It is contemplated that diversified and common data for the validation are to be necessary in order to develop the incoming ion thruster.

[1] Associate Professor, Department of Aerospace Engineering, ynakayam@nda.nda.ac.jp

In order to allowable inspect and validate the numerical analysis codes from diversified perspectives, in this study, a modified two-dimensional visualized ion thruster (VIT_2) is designed and fabricated. Reasons are the follows: (1) two-dimensional ion beam optics can be easily visually measured, (2) many validation can be performed with low cost because two-dimensional numerical simulation cost is lower than three-dimensional simulation cost, (3) the grid current changes can be also obtained, and (4) almost ion beam optics code can easily simulate two-dimensional object because their codes are described in three-dimension.

The objectives of this study are (1) to obtain the ion beam optics data for the validation of numerical simulation, (2) to evaluate the validity with numerical data derived from the igx_2D code simulation, and (3) to release as the common data. The igx_2D is a two-dimensional ion beam optics code.

II. Electrostatic Acceleration Theory

A. One-dimensional Theory [8,9)]

In this section, one-dimensional flow is assumed. Ion thruster grid system has two or three grids: electrodes with many holes. Plasma produced in the discharge chamber, and ion is emitted from the plasma. The ion is accelerated by the electric field of the grid system. The ion current density emitted from the plasma, that is, ion saturation current density, is expressed by the following equation:

$$J_{pi} = \exp\left(-\frac{1}{2}\right) e n_p \sqrt{\frac{kT_e}{M}} \tag{1}$$

This equation is derived from energy conservation, Newton's law of motion, Poisson's equation, and Bohm condition. The ion current density within two electrodes is expressed by the following equation:

$$J_{si} = \frac{4}{9}\epsilon_0 \sqrt{\frac{2e}{M}} \frac{V^{\frac{3}{2}}}{L^2} \tag{2}$$

This equation is the well-known Child's law of space-charge-limited current, and is derived from energy conservation, Newton's law of motion, and Poisson's equation. Assuming that both current densities are same, a length is given by

$$L = \frac{2}{3}\exp\left(\frac{1}{4}\right) \sqrt{\frac{\epsilon_0}{en_p}} \left(\frac{2e}{kT_e}\right)^{\frac{1}{4}} V^{\frac{3}{4}} \tag{3}$$

It is safe to say that this length is the necessary distance to conversion from electrostatic energy to kinetic energy. This is described as "electrostatic acceleration length." This length is larger, as the electric potential gap is increased, and/or as the plasma density is decreased.

B. Two-/Three-dimensional Beam Optics

Since repelling electrostatic forces between ions acts, ion flow is two-/three-dimensional. Figure 1 indicates the schematic of ion flows. These ion flows are called "ion beam optics" because the flows have focal point. These are classified as summarized in Table 1.

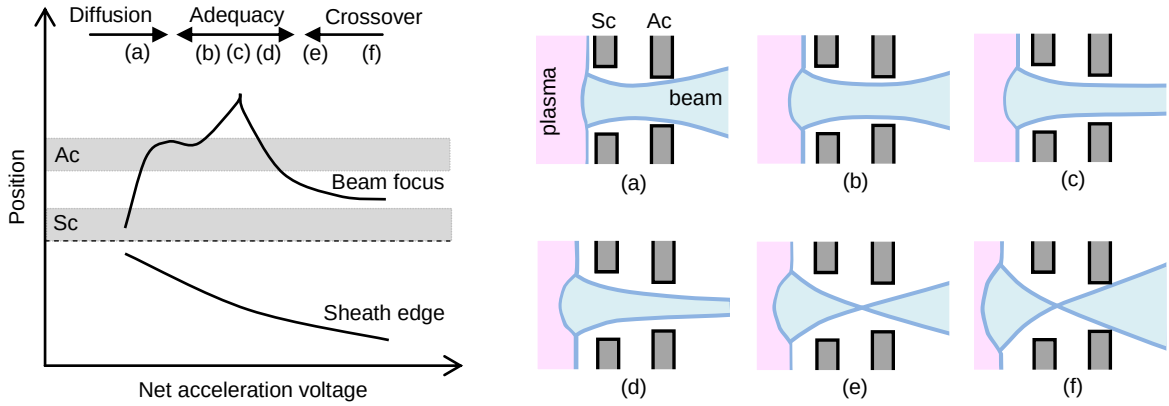

Figure 1 Schematic of plasma sheath and ion beam optics (beam focus and sheath edge position)

Table 1 Ion Beam Optics Type

type	plasma-sheath-shape	beam-shape	beam-focus	impingement
(a)	slightly concave, or convex	diffusion	from Sc to Ac	Yes (diffusion)
(b)	concave	slightly diffusion	near Ac	No
(c)	concave	little diffusion	downstream	No
(d)	concave	conversion	near Ac	No
(e)	concave	crossover	from Sc to Ac	No
(f)	significantly concave	crossover	from Sc to Ac	Yes (crossover)

In case that beam focus is near acceleration grid, it seems that electrostatic acceleration length is almost coincided with focal length. This is because the potential of beam focus is the highest in near acceleration grid hole region.

III. Modified 2-D Visualized Ion Thruster (VIT_2)

A. Ion Source

Figure 2 shows the schematic of the VIT_2. The design of VIT_2 is based on that of the original VIT.[10,11] As depicted in Fig. 2, the VIT_2 is a two-dimensional rectangular parallelepiped. Plasma is produced by direct current discharge: the VIT is an electron-bombardment-type thruster. The discharge chamber wall comprises a pair of L-shaped iron yokes, a pair of rectangle glass plates, and a rectangular stainless steel grid system. The discharge chamber dimensions are 120 mm × 70 mm × 100 mm. Those of the original VIT are 80 mm × 50 mm × 80 mm. The yokes are set for the magnetic field formation; the glass plates are set for the spectroscopic measurements. Two pairs of rectangular stainless steel anodes are set within the discharge chamber. Changing the electrical connection to the upstream anodes or the downstream anodes alters the discharge path. An electron source exists at the center of the upstream discharge chamber wall. The electron is produced by a filament within the source. It is emitted to the discharge chamber through the keeper bridge plasma. The xenon propellant particle flows into the chamber through the electron source. It is ionized by the electron bombardment and extracted by the grid system.

B. Magnetic Field and Baffle

A diffusion-type (Kaufman-type) magnetic field is basically adopted in the VIT_2 discharge chamber. Figure 3 depicts a schematic of the magnetic field, baffle, and primary electron flow. This magnetic field was formed using some Sm-Co permanent magnets. The magnetic field formation is variable because the magnets can be easily demountable. The baffle was set directly at the exit plate of electron source for inclination of the emitted electron flow. The primary electrons emitted from the electron source are inclined to the magnetic force lines by the baffle.

C. Grid System

The grid systems of VIT_2 comprise two grids in this study. Each grid has five narrow slits in the y-direction. The slit width of the screen and the acceleration grid is 6.0 mm and 4.0 mm, respectively. The slit pitch is 10.0 mm. The thickness and slit length of both grids is 1.0 mm and 50.0 mm, respectively. The slits of the viewer's side (in the +y-direction) were canaliform machined to observe most ion beam optics. The remaining thickness is 0.20 mm. The

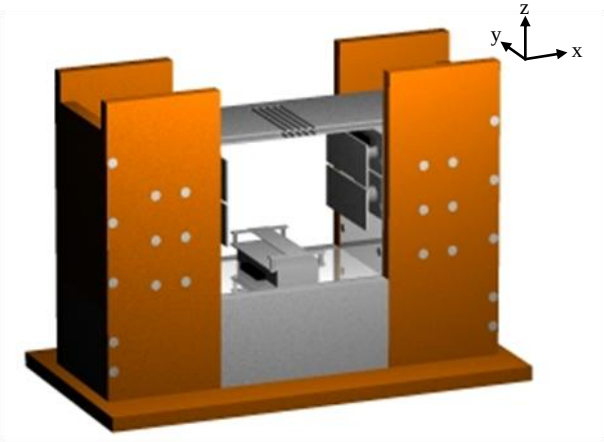

Figure 2 Schematic of VIT_2

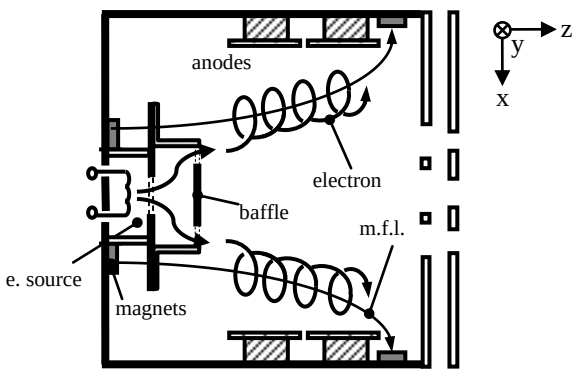

Figure 3 Schematic of discharge in VIT_2

screen grid is fixed to the discharge chamber; the acceleration grid is fitted to the discharge chamber with four stainless steel springs and four ceramic screws to maintain the gap. The gap between the both is 2.0 mm in this study. The slit grid system extracts five sheet-shaped ion beams. A viewer can observe five bright ion beams if seen from the +y-direction.

D. Operation

The electric circuit for the VIT_2 is the essentially same as that for conventional dc electron bombardment ion thruster, except for dual-anode-line. The screen grid is connected electrically to the discharge chamber. The discharge voltage, the anode potential, is 50 V. The VIT_2 operates at the following conditions: propellant flow rate of 0.90 sccm, discharge voltage of 50 V, total discharge current of 0.30 A, and keeper current of 0.10 A, with keeper voltage of 40 V at the off-discharge condition. The keeper voltage instantly decreases to approximately 0 V because of the constant current control at the on-discharge condition. The screen grid potential is 0–2 kV (0.25 kV step); the acceleration grid potential is -500 V. These currents and potentials are applied with errors of 1%. The propellant flow rate control error is less than approximately 1%. The vacuum pressure is approximately 3 mPa when the xenon flow rate is 0.90 sccm (approximately 90 μg/s, Xe). Incidentally, the minimum operable flow rate of the VIT_2 is approximately 0.2 sccm.

E. Measurements

In order to evaluate the ion density distribution of the discharge plasma, fifteen Langmuir probes are used. Each probe is made of 0.20-mm-diameter pure tungsten wire that is almost covered with a 1.0-mm-diameter ceramic tube. The exposed length is 0.08 mm. These probes are directly inserted to the plasma through the grid slits on 5 mm upstream plane from the screen grid on the center axis of the center slit. The location error is less than 1 mm in all directions.

The multi ion beam optics is photographed by a digital camera with a telecentric lens. Since the effective focal distance of the lens is approximately 167 mm, the VIT_2 is set near the observation window of the vacuum chamber. The dimensions of viewing field are approximately 38 mm × 38 mm, and the spatial resolution is approximately 0.014 mm.

F. Performance

Figure 4 shows the discharge plasma and five ion beams observed directly through the VIT_2 glass plate. As described in detail hereinafter, the plasma sheath near the grid system was also observed clearly. The VIT_2 can visualize the schematic of ion production and extraction, as same as the original VIT. The maximal thruster performance of the VIT_2 is the follows: propellant flow rate of 0.25 sccm, total consumption power of 26 W, ion production cost of approximately 600 W/A, propellant utilization efficiency of approximately 56%, specific impulse of approximately 3100 s, and thrust of 0.75 mN.

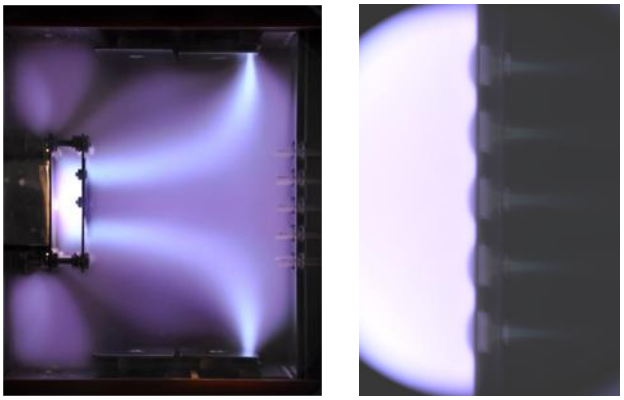

a) discharge plasma **b) five-ion-beam**

Figure 4 Typical photographs

In this investigation, the VIT_2 has the following typical thruster performance: total consumption power of approximately 40 W, ion production cost of approximately 1200 W/A, propellant utilization efficiency of approximately 20%, specific impulse of approximately 1100 s, and thrust of 0.96 mN. The reason of this degradation performance compared to the maximal performance is the flow rate of 0.90 sccm.

G. Plasma Density

The density in the y-direction is almost homogeneously-distributed, and there is a little dip of the x-direction density distribution. At the point of 5 mm upstream from the screen grid of the center slit, the electron number density and electron temperature are approximately 4.5×10^{16} m^{-3} and 4.25 eV, respectively. The plasma space potential in this uniform region is 52–54 V, which is 2–4 V higher than the anode potential. The reproducibility error ratio is approximately 5-10%.

IV. 2-D Ion Beam Optics Code (igx_2D)

A. Numerical Methods

The igx_2D code was based on the igx code. The original igx code simulates ion motion and electric potential field in a three-dimensional cylindrical coordinate system. The igx code simulates with the following methods: (1) energy compensation, (2) simplified definition of plasma pre-sheath, (3) region sharing, (4) flux-tube, (5) particle-in-cell charge distribution, (6) successive-over-relaxation, and (7) object-oriented-coding. The numerical ion motion is described in a Cartesian coordinate system, and the numerical ion charge is distributed to numerical grid points in the cylindrical coordinate system with the region sharing method. The accuracy of the igx code was confirmed with the grid currents behavior of a 19 holes ion thruster. More details of the igx code described in the reference 7.

The igx_2D code simulates ion motion and electric potential field in a two-dimensional Cartesian coordinate system in order to analysis for slit grid system such as that of the VIT and VIT_2. The electric potential field in the igx_2D simulation is calculated with a modified successive-over-relaxation method. This method is preferred over the commonly-used successive-over-relaxation method not only because error accumulation is reduced but also because it requires fewer calculation cost. In addition, the igx_2D code simulates neutralization with simplified definition method of neutralized boundary surface such as above mentioned method.

B. Numerical Conditions

The ion beam optics in the near field of the VIT_2 grid system is calculated. The igx_2D code simulates at the following conditions: numerical node distance of 0.050 mm, potential tolerance of under 0.01 V, calculating area of 86 mm × 18 mm, total cell number of approximately 0.62 million, total flux-tube number of approximately 0.17 million, and 35 iteration loops. The propellant is xenon with temperature of 300 K. The upstream plasma parameters are set in almost accordance with the experimental measured data as mentioned in the section III-G: electron number density of 4.5×10^{16} m^{-3}, electron temperature of 4.25 eV, and plasma space potential of 50 V.

This simulation is performed by a personal computer with the Intel® Core™ 2 processor, and requires approximately 5 minutes per case.

V. Results and Discussion

A. Experimental Validity

Figure 5 shows the grid currents changes against the net acceleration voltage. In case of the voltage of 1.5 kV, the ion beam current density is approximately 0.8 mA/cm^2 (= 12 mA / 5 slit / 0.6 cm / 5 cm). The ion saturation current density derived from Eq. (1) is 0.77 mA/cm^2. Considering that the plasma sheath area is slightly larger than the screen grid slit area, the ion beam current density coincides with the ion saturation current density. Therefore, the plasma measurement in this study was appropriate.

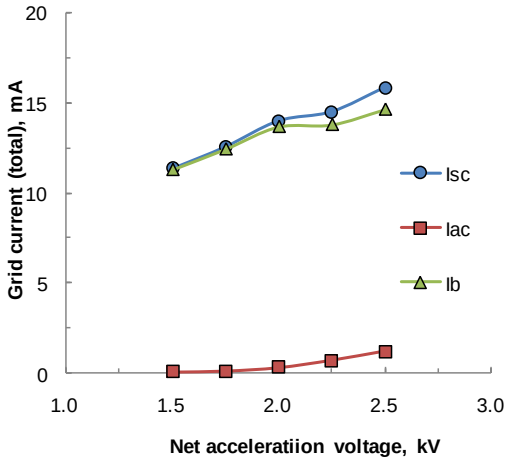

Figure 5 Grid currents

B. Experimental Observed Beam Optics

Figure 6 shows the photographs and weighted images of experimental observed ion beam optics, against the applied grid potential. As shown in the photographs, slightly bright lights are confirmed in the near screen grid and acceleration grid slit region. These are the discharge plasma lights reflected on the slit-end-surfaces of the viewer's opposite side. The weighted images were edited in order to suppress the reflection lights and to emphasize the ion beam optics. The edit process is the follows: (1) conversion from jpeg format to bitmap format (256 shades of RGB, red-green-blue), and (2) subtraction shade level value of the R from shade level value of the B. This is because the xenon neutral luminescence wave length is included in wave length regions of both the R and the B, and the xenon ion luminescence wave length is mainly included in the wave length region of the B.

As shown in this figure, the observed beam optics correspond to the type-(b), (c), and (d) in Fig. 1. In addition, the luminescence intensity of the "rim" is higher than that of the center. These graded beams are confirmed in the numerical simulation results. It may be the first time that the graded beam is experimental observed and confirmed.

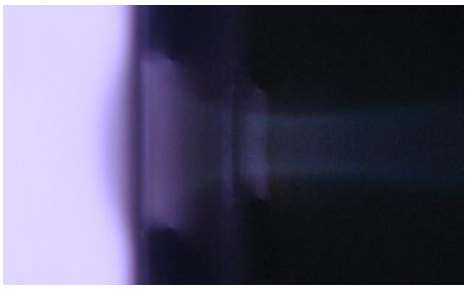

a-1) photograph (1.00 kV / -0.5 kV)

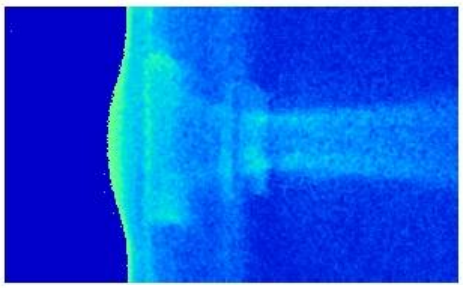

b-1) weighted image (1.00 kV / -0.5 kV)

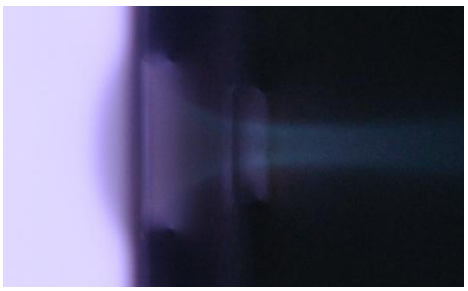

a-2) photograph (1.25 kV / -0.5 kV)

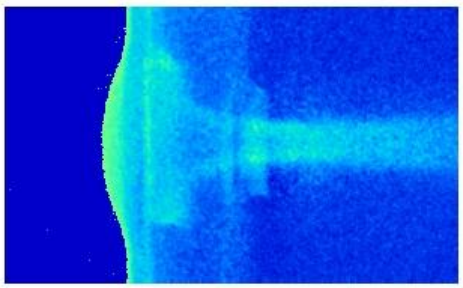

b-2) weighted image (1.25 kV / -0.5 kV)

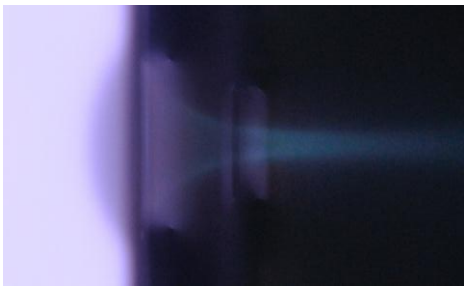

a-3) photograph (1.50 kV / -0.5 kV)

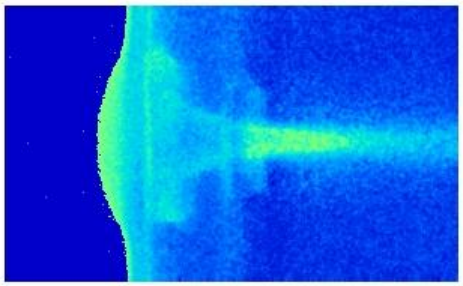

b-3) weighted image (1.50 kV / -0.5 kV)

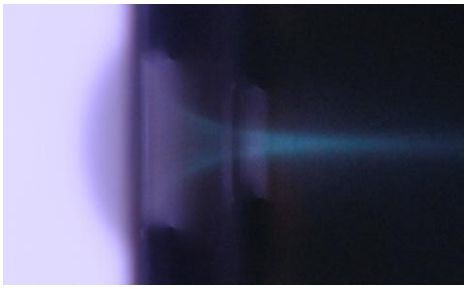

a-4) photograph (1.75 kV / -0.5 kV)

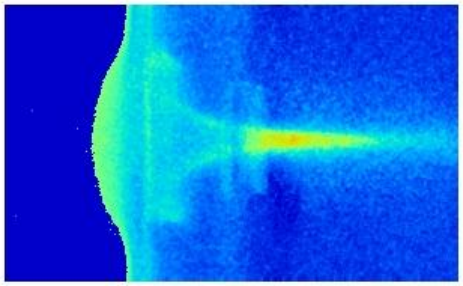

b-4) weighted image (1.75 kV / -0.5 kV)

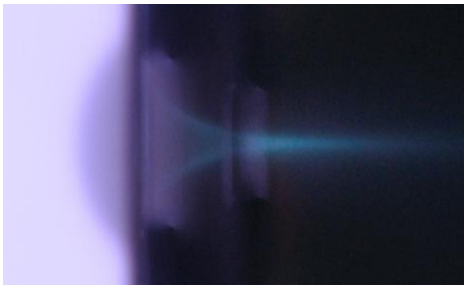

a-5) photograph (2.00 kV / -0.5 kV)

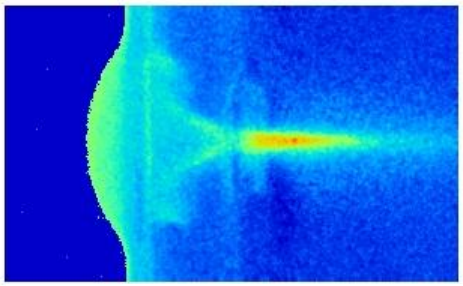

b-5) weighted image (2.00 kV / -0.5 kV)

Figure 6 Ion beam optics against applied grid potential (center slit grid hole)

Figure 7 shows the discretely position data of plasma sheath and ion beam edge. The plasma sheath position was determined as the steep decline point of the luminescence intensity in the upstream region of screen grid. The ion beam edge position was determined as the highest luminescence intensity in the x-direction. The ion beam edge in the near screen grid slit was not determined due to the reflection light.

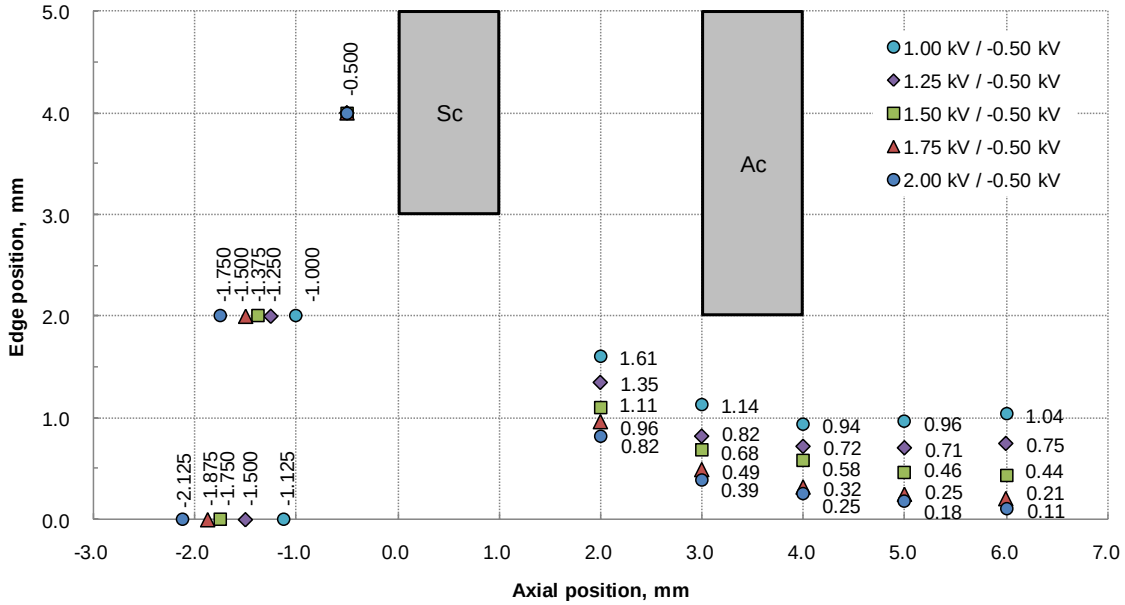

Figure 7 Ion beam edge and plasma sheath edge

C. Plasma Sheath Position and Beam Focus

Figure 8 shows the plasma sheath position and ion beam focus against the net acceleration voltage. The focus was determined as the vertex position of the approximate quadratic function derived from the beam edge position data. The plasma sheath position was determined as the plasma sheath position on the center axis. The numerical data derived from the igx_2D simulation were plotted in this figure. As shown in this figure, the experimental data are in good agreement with the simulated data.

Figure 9 shows the distance between the beam focus and the sheath position against the net acceleration voltage.

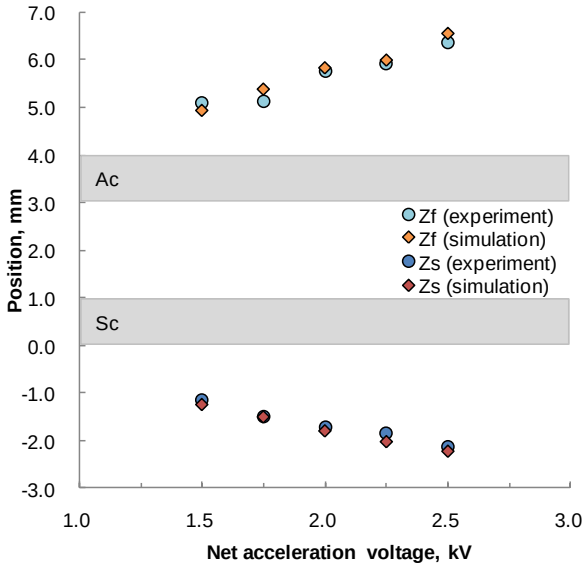

Figure 8 Beam focus and plasma sheath position

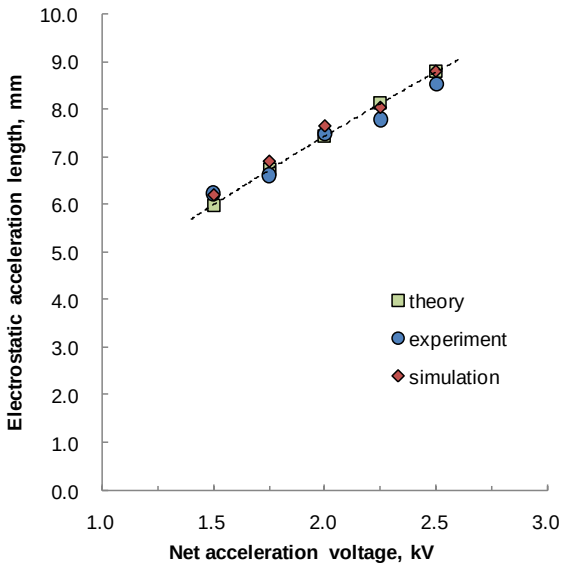

Figure 9 Electrostatic acceleration length

The electrostatic acceleration lengths derived from the Eq. (3) were plotted in this figure. As shown in this figure, the experimental data are in good agreement with not only the simulated data but also the theoretical data.

Considering the coincidence, the experimental observed data as shown in Figs 6 and 7 are useful for the validation of ion beam optics code. If the reflection lights are skillfully deleted, the ion density distribution throughout all regions may be obtained.

VI. Conclusion

The following data necessary to validate ion beam optics simulations from diversified perspectives were experimental obtained in this study:

A) upstream plasma parameters (density, temperature, potential)
B) grid currents
C) plasma sheath shape
D) ion beam optics shape (edge, focus)
E) ion distribution (partly)

The validity of these data was confirmed through the comparison with numerical and theoretical data. Almost ion beam optics code can easily simulate two-dimensional object because their codes are described in three-dimension. Therefore, the experimental data in this paper, especially Figs. 6 and 7, are useful for the validation and for the development of more precise estimation code of ion thruster durability.

Acknowledgments

The author is grateful to Lt. Jun'ichi Iwasaki of Japan Air Self-Defense Force for his helpful assistance. This work was partial supported by KAKENHI 21760661 (Grants-in-Aid for Scientific Research).

References

[1]Whealton, J. H., McGaffey, R. W. and Stirling, W. L. "Ion beam extraction from a plasma with aberration reduction by method of mutual exclusion," *Journal of Applied Physics*, Vol. 52, No. 6, 1981, pp. 3787-3790.

[2]Arakawa, Y. and Ishihara, K., "A Numerical Code for Cusped Ion Thruster," *Proceedings of 22nd International Electric Propulsion Conference*, IEPC-91-118, Italy, 1991.

[3]Free, B., Owens, J. R. and Wilbur, P., "Variations of triple-grid geometory and potentials to alleviate accel grid erosion, *Proceedings of 22nd International Electric Propulsion Conference*, IEPC-91-120, Italy, 1991.

[4]Hayakawa, Y.: Three-Dimensional Numerical Model of Ion Optics System, *Journal of Propulsion and Power*, Vol. 8, No. 1, 1992, pp. 110-117.

[5]Nakano, M. and Arakawa, Y., "Ion Thruster Lifetime Estimation and Modeling Using Computer Simulation," *Proceedings of 26th International Electric Propulsion Conference*, IEPC-99-145, Japan, 1999, pp. 797-804.

[6]Okawa, Y. and Takegahara, H., "Particle Simulation on Ion Beam Extraction Phenomena in an Ion Thruster," *Proceedings of 26th International Electric Propulsion Conference*, IEPC-99-146, Japan, 1999, pp. 805-812.

[7]Nakayama, Y., and Wilbur, P., "Numerical Simulation of Ion Beam Optics for Multiple-Grid Systems," *Journal of Propulsion and Power*, Vol. 19, No. 4, 2003, pp. 608-613.

[8]Jahn, R. G., *Physics of Electric Propulsion*, 1st ed., McGraw-Hill, New York, 1968, Chap. 7.

[9]Lieberman, M. A., *Principle of Plasma Discharges and Materials Processing*, John Wiley & Sons, New York, 1994, Chap. 6.

[10]Nakayama, Y. and Teraura, Y., "Feasibility Study on Visualized Ion thruster," *Proceedings of 30th International Electric Propulsion Conference Paper*, IEPC-2007-043, Italy, 2007.

[11]Nakayama, Y., "Experimental Visualizationof Ion Thruster Discharge and Beam Extraction," *Transactions of JSASS Space Technology Japan*, Vol. 7, No. ists26, Pb_26-Pb_34, 2009.